HHS Public Access

Author manuscript

Cancer Res. Author manuscript; available in PMC 2021 June 28.

Published in final edited form as:

Cancer Res. 2017 July 15; 77(14): 3802–3813. doi:10.1158/0008-5472.CAN-16-2794.

NEMO, a transcriptional target of estrogen and progesterone, is linked to tumor suppressor PML in breast cancer

Kelli E. Valdez[1,*], **Hanan S. Elsarraj**[2,*], **Yan Hong**[3], **Sandra L. Grimm**[4], **Lawrence R. Ricci**[5], **Fang Fan**[6], **Ossama Tawfik**[7], **Lisa May**[8], **Therese Cusick**[9], **Marc Inciardi**[10], **Mark Redick**[11], **Jason Gatewood**[12], **Onalisa Winblad**[13], **Susan Hilsenbeck**[14], **Dean P. Edwards**[15], **Christy Hagan**[16], **Andrew K. Godwin**[17], **Carol Fabian**[18], **Fariba Behbod**[19]

Kelli E. Valdez: kvaldez@kumc.edu; Hanan S. Elsarraj: helsarraj@kumc.edu; Yan Hong: yhong@kumc.edu; Sandra L. Grimm: sgrimm@bcm.edu; Lawrence R. Ricci: Lawrence.Ricci@tmcmed.org; Fang Fan: ffan@kumc.edu; Ossama Tawfik: otawfik@kumc.edu; Lisa May: lisasmay@cox.net; Therese Cusick: tcusick@wsspa.com; Marc Inciardi: minciardi@kumc.edu; Mark Redick: mredick@kumc.edu; Jason Gatewood: jgatewood@kumc.edu; Onalisa Winblad: owinblad@kumc.edu; Susan Hilsenbeck: sgh@bcm.edu; Dean P. Edwards: deane@bcm.edu; Christy Hagan: chagan@kumc.edu; Andrew K. Godwin: agodwin@kumc.edu; Carol Fabian: cfabian@kumc.edu

[1]Department of Pathology and Laboratory Medicine, The University of Kansas Medical Center, 3901 Rainbow Blvd, Kansas City, KS, 66160

[2]Department of Pathology and Laboratory Medicine, The University of Kansas Medical Center, 3901 Rainbow Blvd, Kansas City, KS, 66160

[3]Department of Pathology and Laboratory Medicine, The University of Kansas Medical Center, 3901 Rainbow Blvd, Kansas City, KS, 66160

[4]Department of Molecular & Cellular Biology, Pathology & Immunology, One Baylor Plaza, Houston, Texas 77030

[5]Department of Radiology, Truman Medical Center, 2301 Holmes Street, Kansas City, MO 64108

[6]Department of Pathology and Laboratory Medicine, The University of Kansas Medical Center, 3901 Rainbow Blvd, Kansas City, KS, 66160

[7]Department of Pathology and Laboratory Medicine, The University of Kansas Medical Center, 3901 Rainbow Blvd, Kansas City, KS, 66160

[8]Department of Radiology, The University of Kansas School of Medicine-Wichita, 1010 N. Kansas, Wichita, KS, 67214

[9]Department of Surgery, The University of Kansas School of Medicine-Wichita, 1010 N. Kansas, Wichita, KS, 67214

[10]Department of Radiology, The University of Kansas Medical Center, 3901 Rainbow Blvd, Kansas City, KS, 66160

[11]Department of Radiology, The University of Kansas Medical Center, 3901 Rainbow Blvd, Kansas City, KS, 66160

[19]Corresponding author and requests for reprints: Fariba Behbod, Department of Pathology and Laboratory Medicine, MS 3045, The University of Kansas Medical Center, Kansas City, KS, 66160, Tel: (913) 945-6642, Fax: (913) 945-6838, fbehbod@kumc.edu.

[*]Kelli E. Valdez and Hanan S. Elsarraj contributed equally to this manuscript as first authors.

Disclosure of potential conflict of interest: The authors declare no potential conflicts of interest.

[12]Department of Radiology, The University of Kansas Medical Center, 3901 Rainbow Blvd, Kansas City, KS, 66160

[13]Department of Radiology, The University of Kansas Medical Center, 3901 Rainbow Blvd, Kansas City, KS, 66160

[14]Smith Breast Center, Baylor College of Medicine, One Baylor Plaza, Houston, Texas 77030

[15]Department of Molecular & Cellular Biology, Pathology & Immunology, One Baylor Plaza, Houston, Texas 77030

[16]Department of Biochemistry, The University of Kansas Medical Center, 3901 Rainbow Blvd, Kansas City, KS, 66160

[17]Department of Pathology and Laboratory Medicine, The University of Kansas Medical Center, 3901 Rainbow Blvd, Kansas City, KS, 66160

[18]Department of Medicine, Breast Cancer Survivorship Center, The University of Kansas Medical Center, 3901 Rainbow Blvd, Kansas City, KS, 66160

Abstract

The beneficial versus detrimental roles of estrogen plus progesterone (E+P) in breast cancer remains controversial. Here we report a beneficial mechanism of E+P treatment in breast cancer cells driven by transcriptional upregulation of the NFκB modulator NEMO, which in turn promotes expression of the tumor suppressor protein PML. E+P treatment of patient-derived epithelial cells derived from ductal carcinoma in situ (DCIS) increased secretion of the pro-inflammatory cytokine IL-6. Mechanistic investigations indicated that IL-6 upregulation occurred as a result of transcriptional upregulation of NEMO, the gene for which harbored estrogen receptor (ER) binding sites within its promoter. Accordingly, E+P treatment of breast cancer cells increased ER binding to the NEMO promoter, thereby increasing NEMO expression, NFκB activation and IL-6 secretion. In two mouse xenograft models of DCIS, we found that RNAi-mediated silencing of NEMO increased tumor invasion and progression. This seemingly paradoxical result was linked to NEMO-mediated regulation of NFκB and IL-6 secretion, increased phosphorylation of STAT3 on Ser727 and increased expression of PML, a STAT3 transcriptional target. In identifying NEMO as a pivotal transcriptional target of E+P signaling in breast cancer cells, our work offers a mechanistic explanation for the paradoxical anti-tumorigenic roles of E+P in breast cancer by showing how it upregulates the tumor suppressor protein PML.

Keywords

DCIS; estrogen; progesterone; NEMO; PML

Introduction

Ductal carcinoma in situ (DCIS) is a non-obligate precursor of invasive ductal carcinoma (IDC) and is diagnosed in more than 60,000 women a year in the United States annually and rising (1). Treatment consists of either lumpectomy, often combined with radiation therapy, or mastectomy (2). However, not all lesions described as DCIS follow a clinical course that

supports such invasive treatment. Long-term follow up studies of misdiagnosed and untreated DCIS have reported an average rate of progression of 43% (24–75%) (3). These included all histologic types such as comedo as well as non-comedo and papillary DCIS (3). The mechanisms regulating the transition of DCIS to IDC are critical but remain as an understudied area. We have developed a novel xenograft model in which DCIS cells can be engrafted within the mammary ducts of immunodeficient mice, allowing the study of potential regulators of DCIS invasive progression (4). The role of estrogen and progesterone (E+P) exposure and risk of breast cancer is controversial. Events that result in longer lifetime exposure to hormones estrogen and progesterone have been shown to increase a woman's relative risk of getting breast cancer (5–11). However, the mechanisms underlying this association are still unclear.

Previous studies have revealed the protective role for E+P in mammary tumorigenesis. Medina and colleagues, using the *p53*-null mammary transplant model, showed that a short 2-week exposure to E+P during the immediate post-pubertal stage of mammary development decreased mammary tumorigenesis by 70 to 88% (12). The Carroll laboratory has recently published a provocative study in which they showed that not only is progesterone receptor (PR) recruited to the estrogen receptor (ER) complex to affect the transcriptome, but it actually inhibits ER-stimulated growth, going against the dogma that hormonal exposure increases breast cancer risk (13,14). In the current study, we report a beneficial mechanism of E+P treatment in breast cancer cells driven by transcriptional upregulation of the NFκB modulator NEMO, which in turn promotes expression of the tumor suppressor protein PML.

Methods

Specimen collection

All patients gave written informed consent for participation in this University of Kansas Medical Center IRB-approved study allowing collection of additional biopsy and or surgical tissue for research. Subject recruits included patients undergoing image-guided core needle biopsy or surgical excision (lumpectomy or mastectomy) due to suspicion of DCIS. In all cases, research specimens were obtained only after acquisition of diagnostic specimens. Following collection, biopsy tissue was placed in preservation media (LiforCell, *Life*blood Medical, Inc., Freehold, NJ) and stored at 4°C on ice until processing as previously described to isolate the epithelial and stromal cell components (4).

Cell culture

MCF7 and BT474 were a gift from Dr. Roy Jensen's laboratory (University of Kansas Medical Center, Kansas City, KS) obtained from ATCC. Cell lines authentication with Short Tandem Repeat (STR) finger printing was performed by Cell Characterization Core at MD Anderson in September 2015. DCIS.com ER/PR+ cell was a gift from Dr. Dean Edwards and cell authentication with STR was performed by Cell Characterization at MD. Anderson. DCIS.com cells were engineered to stably express ER and PR-B with lentiviral vectors using an EF1α promoter and an IRES-ZsGreen or IRES-dTomatoRed tag (15), enabling the isolation of a mixed population of receptor-positive cells by flow cytometry. All cell lines were mycoplasma tested and were negative.

Animals and transplantation

Recipients were 8- to 10-week-old virgin female NOD-SCID IL2Rgamma^{null} (NSG) mice, which were purchased from Jackson Laboratories. Animal experiments were conducted following protocols approved by the University of Kansas School of Medicine Animal Care and Use and Human Subjects Committee. A 30-gauge Hamilton syringe, 50-μl capacity, with a blunt-ended 1/2-inch needle was used to deliver the cells as previously described (16). Two μl of PBS (with 0.04% trypan blue) containing 10,000 cells were injected. At the time of intraductal transplantation surgery, a 1 cm incision is made between the scapulae and a pellet containing estrogen and progesterone is inserted subcutaneously. After 6 to 8 weeks, mice were sacrificed and the mammary glands harvested and fixed in 4% paraformaldehyde on ice for 2h. Mammary tissue was processed for embedding as previously described and sectioned at 5μm (16).

To make hormonal pellets, silastic medical grade tubings (Dow-Corning 241557) were sterilized and sealed at one end with medical adhesive silicone glue (Fisher NC9186391) and left to dry for 3 hours. Then 4mg of (1:79) estradiol (Sigma E8875-1G) /cholesterol (Sigma C75209-25G) mixture and 20 mg progesterone (Sigma P0130-25G) were added to 0.25 cm and 1cm length tubes, respectively.

NFκB p65 activity

MCF7, BT474, and DCIS.com cells were serum-starved for 24h before treatment with 10nM E and 10nM P. Nuclear extract was collected 48h later using Active Motif's Nuclear Extract kit (Active Motif 40010), and the TransAM® NFκB Transcription Factor Assay (Active Motif 43296) was used to measure active NFκB p65 within 25μg of nuclear extract following the manufacturer's recommendations.

IL-6 secretion

MCF7, BT474 and DCIS.com cells were serum-starved for 24 h before treatment with 10nM E and 10nM P. Cell culture media was collected 48h later and the Quantikine® ELISA Human IL-6 Immunoassay (RnDSystems D6050) was used to measure IL-6 secretion following the manufacturer's recommendations.

In vivo invasion studies

NEMO KD, and scrambled shRNA control (control) MCF7 and ER+/PR+ DCIS.COM cells were injected at 10,000 cells per gland. A total of four glands and three animals were used for each group. The glands were collected at 6 and 8 weeks post-intraductal injection in MCF7 and ER+/PR+ DCIS.com xenografts, respectively. The mammary glands containing DCIS lesions were then fixed, embedded and sectioned and were prepared for IF as described above. Measurement of maximum distance of invasion and number of invasive areas were performed as previously described (17).

Results

Hormones (E+P) promote increased mammosphere formation efficiency of primary epithelial and stromal cells derived from ER^+PR^+ DCIS

DCIS tissues were collected from consented patients undergoing image-guided core needle biopsy or surgical excision due to suspicion of DCIS. Following tissue digestion, epithelial cells from primary human DCIS were cultured under non-adherent conditions, encouraging mammosphere formation, in the presence of vehicle or 10nM estradiol (E) and 100nM progesterone (P). It is important to note that while the overnight digestion of DCIS patient samples yields an enriched population of epithelial cells (~90%), the remaining are stromal fibroblasts (~10%) (data not shown). A subset of cases (termed “responders”) responded to the steroid hormone treatment *in vitro* by increasing mammosphere-forming efficiency in E+P conditions compared to vehicle control (Fig. 1 and Supplementary Table. S1; cases 1–6 are non-responders and cases 7–11 are responders). Supplementary Table. S1 also contains two cases of non-responders (12,13) and three cases of responders (14–16). Mammosphere efficiency was calculated as the ratio of secondary to primary mammospheres, and presented as the fold-change in E+P-treated over the vehicle-treated control (Fig. 1A). As shown in Supplementary Table. S1, there were no differences between the responders and non-responders with respect to many of the available patient data including the percentage of ER and PR expression. Not finding a significant correlation may be due to a small sample size included in this study.

We then examined cellular composition of mammospheres by utilizing epithelial specific markers, cytokeratin (K)-5 plus K-19, and a fibroblast marker, fibroblast specific protein 1 (FSP1). To our surprise, some mammospheres contained FSP positive (FSP^+) fibroblasts only and referred to as FSP+ spheres, some contained K^+ epithelial cells only and referred to as K+ spheres, and some contained both $K5/19^+$ and FSP^+ fibroblasts referred to as mixed spheres (Fig. 1B). As shown in Fig. 1C, while E+P exposure increased sphere formation efficiency by both cell types (FSP^+, K^+ and mixed), only FSP^+ spheres showed a significant increase in sphere formation efficiency in response to E+P. However, all three sphere types contributed equally to the total number of spheres counted in each sample. These data indicate that both cell types form spheres and contribute to the total number of spheres counted in our mammosphere cultures.

E+P treated cases that exhibited increased mammosphere formation efficiency showed a significant increase in IL-6 secretion

We investigated the role of IL-6 in mammosphere formation efficiency since a number of studies have shown IL-6 to be a direct regulator of breast cancer stem cell self-renewal and to promote breast cancer tumorigenesis, angiogenesis and metastasis (18–21). However, there are also studies, which demonstrate the growth inhibitory role of IL-6, in particular, during early stages of cancer progression in melanoma, prostate and breast cancer (22,23). To investigate whether IL-6 is associated with an increase in E+P increased DCIS mammosphere formation efficiency, primary human DCIS cells collected from patient biopsies were cultured under non-adherent conditions with vehicle control or estradiol (10nM; E) and progesterone (100nM; P). After 10 days primary mammospheres were

counted, trypsinized to single cells and re-plated to allow secondary mammospheres to form for 10–14 days. Mammosphere-forming efficiency was calculated as the ratio of secondary to primary mammospheres, normalized for the number of cells plated. We examined IL-6 secretion into cell culture media in 3 non-responding DCIS cases and 1 responding case. Representative cases shown in Fig. 2A and B, demonstrated that IL-6 increased only in the responding DCIS case (*i.e.*, a case in which E+P increased mammosphere formation efficiency; Fig. 2 right A and B), while in DCIS that decreased mammosphere efficiency in response to E+P, IL-6 also decreased (Fig. 2 left A and B; *P<0.05 compared to vehicle control). We performed mammosphere efficiency and IL-6 expression assay by ELISA on five more cases of ER/PR positive DCIS. The data, included as Supplementary Figures. S1A and B, show that three of the five cases showed increased mammosphere efficiency in response to E+P (A) and the same cases also showed a significant increase in IL-6 production (B). In summary our results indicate that IL-6 secretion is significantly increased in DCIS cells that also show a significant increase in mammosphere formation efficiency in response to E+P treatment.

IL-6 expression is higher in DCIS with associated IDC compared to pure DCIS

Tissue microarrays constructed with tissue from patients with either pure DCIS or DCIS with associated IDC were analyzed for IL-6 expression. The lowest expression of IL-6 was found in DCIS cells from patients with no invasive component (Fig. 2C–D; *P<0.01). Comparatively, IL-6 expression was higher in DCIS cells from patients that also had areas of IDC. Within this patient population, the areas of IDC contained higher IL-6 compared to the DCIS component (Fig. 2C and E; *P<0.01). These data indicate that IL-6 expression is increased in DCIS with invasive component.

The NFkB regulator, NEMO, is transcriptionally controlled by E+P

NEMO, a known activator of NFκB signaling, is an established stimulator of IL-6 expression. In a search to identify a link between E+P treatment and IL-6 secretion, we found that the *IKBKG* gene, which encodes NEMO contains a potential binding site for ER (motifmap.ics.uci.edu; searched using the human hg18 multiz28way_placental data base for ESR1 binding sites. In motifmap.ics.uci.edu web tool, we searched for ESR1 binding motifs in target genes. This analysis showed ESR1 binding motif in 2461 genes. We then performed an analysis in IPA (Ingenuity Pathway Analysis) and found that among the 2461 genes, 20 genes were involved in the NFκB pathway. Supplementary Table. S2 includes the 20 ER targets and their role in NFκB pathway. We chose to focus on IKKγ because, ESR1 binding motif to IKKγ showed a false discovery rate (FDR) of 0.05% and was found to directly regulate the activation of NFκB signaling. FDR is the median number of sites discovered for the control motifs divided by the number of sites discovered for the known motif (24).

Insight into the essential role of NEMO in NFκB activation has been gained through observations of individuals with hypomorphic X-linked recessive mutations in the gene encoding NEMO, which leads to ectodermal dysplasia and immunodeficiency (25). In primary patient cells stimulated with E+P, we found that NEMO and IL-6 expression increased in ER^+PR^+ DCIS, but not atypical ductal hyperplasia cells (Fig. 3A). Furthermore, in ER^+PR^+ breast cancer cell lines cultured as monolayers for 12 hours in the presence of

vehicle, E (10nM), P (100nM), or E+P, NEMO gene expression was stimulated in response to E+P (Fig. 3B). Interestingly, in both T47D and BT474 cells, treatment with P alone was sufficient to stimulate NEMO gene expression. To test the ability of ER to bind to the *IKBKG* promoter, we performed chromatin immunoprecipitation assays on MCF7 cells treated with vehicle, E (10nM), P (10nM), or E+P for 1h. For all subsequent studies, we used P at 10nM since we found no significant difference between P at 10 and 100nM concentration with respect to E+P induced upregualtion of NEMO gene expression by qPCR in primary DCIS cells (Supplementary Fig. S1D and E). Immunoprecipitation was performed using an anti-ER antibody and qPCR was performed using primers targeting the potential ERE within the *IKBKG* promoter region. Interestingly, E or P treatment alone did not facilitate ER binding, while E+P treatment led to a 7-fold increase in ER binding to the *IKBKG* promoter region compared to IgG control (Fig. 3C; mean ± SEM; *P< 0.05). ChIP analysis on cells derived from a case of DCIS with associated IDC cells with high expression of ER and PR (95% and 75%, respectively) also showed a 3-fold increase in ER binding to *IKBKG* promoter with E+P treatment (Fig. 3D; mean ± SEM; *P <0.05). However, a chip analysis on cells derived from 3 DCIS patients showed no increase in ER recruitment with hormone treatment (Data not shown). This may be because, while ER expression was high in these three patients (99–100%), PR expression was relatively low (15–22%). These data suggest that the binding of ER to the *IKBKG* promoter may require high-level expression of both ER and PR. However, to prove the role of PR, PR levels will need to be modified and shown to be significantly correlated with NEMO gene expression in response to E+P.

NEMO is required for NFκB activation and IL-6 secretion in response to E+P

In order to explore the role of NEMO in E+P driven DCIS progression, we used targeted shRNAs to knockdown NEMO expression in MCF7 and BT474 cells (Fig 4A). Following 48h treatment with E+P, nuclear extract and cell culture media were collected to measure active NFκB p65 and IL-6 secretion, respectively. E+P treatment increased active NFκB p65 and IL-6 secretion in non-silencing control but not NEMO-KD ER^+PR^+ MCF7 cells (Fig. 4B–C; P<0.05). Interestingly, ER^+PR^+ $HER2^+$ BT474 cells can activate NFκB in the absence of NEMO, indicating that these cells may utilize the non-canonical pathway of NFκB activation which is dependent upon IKKα activation in the absence of IKKβ and NEMO (26). Furthermore IL-6 secretion was consistently elevated in BT474, compared to MCF7 cells, indicating that in these cells IL-6 may not be E+P or NFκB dependent. In order to confirm our results in a DCIS cell line, we utilized ER+/PR+ DCIS.com cells. This cell line has been generated in the laboratory of Dr. Dean Edwards at Baylor College of Medicine by over-expression of ER and PRB (herein referred to as ER+/PR+DCIS.com) by lentiviral transduction. ER+/PR+ DCIS.com cells show a significant induction of ER target genes including GREB1 and TFF1 (unpublished results). Normally, DCIS.com is a triple negative cell line that generates basal DCIS like lesions *in vivo* when transplanted by the intraductal method (16). As seen in Supplementary Fig. S2A and B, ER+/PR+ DCIS.com cells showed a significant increase in NEMO mRNA expression in response to E+P treatment as assessed by qPCR and at the protein level as assessed by Western blot. Furthermore, ER+/PR+ DCIS.com transduced with shRNA to knockdown NEMO showed a reduction in NEMO protein expression (Supplementary Fig. S2B) and in IL-6 production at

baseline and in response to E+P treatment (Supplementary Fig. S2C). These data indicate that, in contrast in MCF7 and BT474 cells, NEMO plays a role in both the baseline as well as E+P induced IL-6 secretion in these cells. E+P treatment of cells resulted in a non-significant increase in NFκB activation in ER+/PR+ DCIS.com cells, while in these cells the baseline and E+P induced NFκB activation did not significantly change with NEMO-KD (Supplementary Fig. S2D). Despite these results, ER+/PR+ DCIS.com still showed a significant increase in IL-6 secretion in response to E+P treatment (Supplementary Fig. S2C; compare a vs. b) and NEMO-KD cells showed significantly reduced baseline level as well as E+P induced IL-6 production (Supplementary Fig. S2C; compare a vs. c and b vs. d). These data suggest that NEMO regulation of IL-6 may be independent of NFκB activation in these cells. Indeed, in some cells, NEMO may regulate IL-6 production, independent of NFκB, through activation of receptor-interacting protein kinase 1 (RIPK1) (27,28).

NEMO knockdown DCIS lesions showed increased in vivo invasive progression

To examine the effect of NEMO-KD on DCIS progression, we utilized the mouse-intraductal (MIND) model. MIND is a novel model in which human breast cancer cells are injected intraductally and studied over time in immunocompromised mice. The MIND model is particularly innovative because, in contrast to other *in vivo* models of breast cancer, in the MIND model human breast cancer cells are actually transplanted into mouse mammary ducts, the same location as they develop in humans, instead of being placed into cleared fat pads outside the mammary ductal system. The MIND xenografts initially form *in situ* lesions followed by progression to invasion as they bypass the mouse mammary ducts and the basement membrane (Fig. 5A).

MIND xenografts were created using NEMO-KD MCF7 and ER+/PR+ DCIS.com cells as well as the control cells followed by mammary gland excision 6 and 8 weeks post-intraductal transplantation, respectively. Both cell lines showed a significant increase in invasive progression with NEMO-KD compared to the control groups (Fig. 5B–E). Additionally, there was a significant increase in *in vitro* cell survival and proliferation in MCF7 NEMO-KD cells compared to control (Supplementary Fig. S3 A–D), while these values did not reach statistical significance in ER/PR+ DCIS.com cells (data not shown).

A search for a clue to these unexpected results led to a link between NEMO and IL-6/STAT3 signaling as well as a STAT3 transcriptional target, tumor suppressor protein promyelocytic leukemia (PML). PML is a founding member of a growing family of proteins that contain a distinctive C3HC4 zinc finger domain termed RING (really interesting gene). Another prominent member of this RING domain containing family is BRCA1 known for its role in tumor suppression and genomic stability (29). PML is critical for the formation and stability of PML nuclear bodies (PML-NBs), macromolecular sub-nuclear structures implicated in tumor suppression functions including apoptosis, growth arrest and cellular senescence (29). Recently, it has been shown that IL-6 signaling represents an important regulator of PML nuclear expression (23). In this study, NEMO-KD was associated with down regulation in NFκB activity, suppression in IL-6 and phospho-STAT3 expression, and a decrease in PML mRNA and protein levels (23). Indeed, STAT3 activated transcription of PML by directly binding to the promoter region of PML (23). We also evaluated the effect of NEMO-KD on

the expression of RIPK1. NEMO has been shown to bind to and stabilize RIPK1 by preventing Lys48 linked RIPK1 ubiquitination and degradation. (28). RIPK1 plays a dual role in cell survival and cell death (28,30,31). RIPK1 can promote cell death through the activation of caspase 8 and/or JNK. RIPK1 can also promote cell survival and proliferation through the activation of MAPK and NFκB pathways (28). Therefore, RIPK1 functions as a hub, where a decision is made for both cell survival and cell death depending on the cellular context and a balance in RIPK1 binding partners. We reasoned that NEMO-KD might push the balance towards RIPK1 mediated cell proliferation and survival. Therefore, we proceeded with examining the expression of IL-6, pSTAT3^{Ser727} (phosphorylated serine 727), PML, and RIPK1 in MCF7 and ER+/PR+DCIS.com MIND xenografts with and without NEMO-KD. These studies showed that NEMO-KD MCF7 xenografts when compared to control showed a significant reduction in IL-6 (Fig. 6A [a. vs. b.] and Fig. 6B [a]), pSTAT3^{Ser727} (Fig. 6A [c. vs. d] and Fig. 6B [b]), and PML (Fig. 6A [e. vs. f] and Fig. 6B [c]). NEMO-KD cells also showed a non-significant increase in RIPK1 (Fig. 6A [g. vs. h.] and Fig. 6B [d]) and a significant increase in expression of Phospho-p44/42 MAPK (pERK) (Fig. 6A [i. vs. j.] and 6B [e.]) two oncogenic proteins known to also be regulated by NEMO (28,30). We repeated these results in ER+/PR+ DCIS.com and showed that NEMO KD was also associated with a significant reduction in IL-6, pSTAT3^{Ser727} and PML (Supplementary Fig S4A and B) expression. These studies indicate that NEMO-KD is associated with a reduction in PML and this may be through the regulation of NFκB/IL-6/STAT3 signaling. NEMO-KD induced PML down regulation represents one mechanism by which NEMO-KD xenografts showed higher *in vivo* tumorigenicity. Since over expression of RIPK1 has been shown to promote melanoma cell proliferation (4) and we have observed a non-significant increase in RIPK1 with NEMO-KD, we can not rule out the possibility that an imbalance in the expression of RIPK1 played a role in NEMO-KD induced tumorigenicity.

While, we have focused on DCIS in this study, the NEMO protective pathway may also have relevance to invasive breast cancers. Our analysis of the Kaplan Meier Plotter in invasive breast cancers showed that higher NEMO mRNA expression was associated with higher recurrence free survival (RFS) in all breast cancers including luminal A and luminal B breast cancers. Similar to NEMO, higher PML was also associated with higher RFS in all breast cancers including luminal A and B breast cancers. Interestingly, higher PML was also associated with higher overall survival in all breast cancers (32) (Supplementary Fig. S5 and Supplementary Table. S3).

Discussion

Our experiments showed that those DCIS epithelial cells that responded to E+P by increased mammosphere formation efficiency also showed high level expression of IL-6 secretion in the culture medium. Since a link between E+P and IL-6 had not been shown previously, we searched transcription binding site databases and found that the IKBKG gene, which encodes NEMO, contains several potential ER binding sites. Indeed, ChIP analysis on several primary DCIS samples and ER/PR positive cell lines showed that, upon E+P treatment, ER bound to the NEMO promoter only in high ER/PR expressing patient samples and breast cancer cell lines. E+P treatment was also associated with increased expression of

NEMO at the protein and RNA levels, activation of NFκB and IL-6 secretion. Since NEMO is a known activator of NFκB signaling and IL-6 secretion, our results indicate that NEMO may serve as a link between E+P signaling and IL-6 secretion in breast epithelial cells. Since, previous studies had shown IL-6 to be a direct regulator of breast CSC self-renewal and to promote breast cancer progression (18–21), we expected NEMO-KD to prevent DCIS invasive progression. On the contrary, NEMO-KD resulted in an unexpected increase in cellular proliferation, survival and in vivo invasive progression of DCIS xenografts.

Role of NFκB essential modulator (NEMO) in tumorigenesis

NEMO is the regulatory subunit of the IKK (inhibitor of NF-kappa-B kinase) core complex, which phosphorylates the inhibitor of NF-kappa-B (IκB) thus promoting the dissociation of the IκB and ultimately degradation of the inhibitor and subsequent activation of NFκB signaling. While NFκB signaling is known for its role in inflammation and innate immunity, it is also recognized as a crucial player in cancer promotion including breast cancer (33,34). A search for a mechanism by which a knockdown in NEMO, an activator of NFκB signaling, could promote tumor progression led to two possible scenarios. First, NEMO may regulate the stabilization of RIPK1, a kinase known to play a role in directing a cell's decision to live or die (28,31). RIPK1 functions as a hub, where a decision is made for both cell survival and death dependent on the cellular context and a balance in RIPK1 binding partners. Our studies showed that NEMO-KD resulted in a non-significant increase in RIPK1 and a significant increase in phosphor-ERK expression. While, the mechanism by which NEMO-KD would result in an increase in RIPK1 protein expression is not clear, overexpression of RIPK1 has been shown to promote melanoma cell proliferation and anchorage independent growth (31). Therefore an imbalance in the expression levels of RIPK1 could still provide an explanation for higher tumorigenicity of NEMO-KD cells.

NEMO regulation of PML represents another possible mechanism for its anti-tumorigenic effects in breast cancer

NEMO is a known activator of NFκB signaling and IL-6 secretion. IL-6 receptor activation induces JAK/STAT3 signaling. Both serine and tyrosine phosphorylated STAT3 have been shown to play pleotropic roles in normal mammary gland development and oncogenesis (35). A recent study showed that IL-6/STAT3 signaling activates transcription of PML by a direct binding of STAT3 to the PML promoter region (23). While, the role of IL-6/STAT3 signaling in prevention vs. promotion of breast cancer has been debated, STAT3 regulation of PML may represent one mechanism for IL-6 induced tumor suppression.

Protective role of E+P in breast cancer through the regulation of NEMO

The most compelling evidence regarding the risk of breast cancer with hormonal therapy comes from two randomized trials conducted by the National Institutes of Health. These large studies that included 27,000 women ages 50 to 79 showed that E+P was associated with significantly higher risk of breast cancer and the risk increased with the length of time that women took the hormones (36,37). Nurse's Health Study that included 116,000 women between the ages of 24 to 43 years found that those who took oral contraceptives had a slight increase in breast cancer risk. However, the accumulative risk was primarily among women who took the "triphasic" formulation (38). Several groups have demonstrated the ability of E

+P to enhance self-renewal of mammary stem cells and result in cancer progression(39). However, these studies have all utilized models of normal mammary epithelium or IDC, and have not focused on the role of E+P in the critical transition from non-invasive DCIS to IDC.

Despite the above results showing harmful effects of E+P treatment, Carroll laboratory recently demonstrated that PR directed ERα chromatin binding which resulted in the expression of a gene signature associated with good clinical outcome. Furthermore, they showed that progesterone inhibited estrogen mediated growth of ERα positive cell lines and primary ERα positive breast tumor xenografts (13). Further proof of phenotypic antagonism between ER and PR in breast cancer, has been demonstrated by Singhal H and colleagues (40). By utilizing primary ER/PR positive primary breast cancer cells and cell lines, this group showed that each hormone alone, E or P, in isolation regulated the expression of common genes and cellular processes, i.e. cell proliferation. However, in the presence of both hormones, progesterone exerted an anti-estrogenic effects with regards to tumorigenic transcriptome, cellular processes and ER/PR recruitment to genomic sites (40). Other groups have also shown that progesterone treatment prevented the growth of some ER/PR positive breast cancer cell lines as well as patient derived xenografts (41–43). Medina and colleagues, using the *p53*-null mammary transplant model, showed that a 2-week exposure to estrogen and progesterone during the immediate post-pubertal stage of mammary development resulted in a significant decrease in mammary tumorigenesis (12). All together, these results point to the necessity for a closer look at the molecular mechanisms and intracellular signaling molecules regulated by ER/PR signaling vs. ER or PR alone. We propose that NEMO regulation of PML expression may represent one mechanism for ER/PR anti-tumorigenic effects in breast cancer.

Role of PML in tumor suppression

Our studies showed NEMO-KD to result in a significant reduction in PML nuclear expression. This indicates that NEMO, either directly through the regulation of IL-6/STAT3 signaling or indirectly by other unknown mechanisms regulates PML expression and function. The tumor suppressor protein, PML, was originally discovered in Acute Promyelocytic Leukemia (APL), as the fusion partner protein with retinoic acid receptor alpha (RARα). This fusion protein is referred to as PML-RARα (29). Indeed, the formation of PML-RARα has been recognized as the underlying etiology of APL since expression of PML-RARα was sufficient to induce leukemia in transgenic animals, while a dominant negative RARα mutant failed to do so. This reveals the important role of a functional disruption in PML in leukemogeneis (44). PML is the core component of subnuclear structures known as PML nuclear bodies (PML-NBs). PML-NBs are important in cell cycle arrest, survival and apoptosis. Indeed, inactivation or down-regulation of PML has been found in many cancers. A large number of PML protein partners (>120) have been identified to physically interact with PML, and to co-localize with PML-NBs (45). Although, many mechanisms have been proposed, two of such mechanisms include the interaction of PML with p53 facilitating its transcriptional activation, and PML cooperation with pRB in formation of senescence-associated heterochromatin foci (46). In conclusion, our studies reveal a novel mechanism by which E+P may protect against aggressive breast cancer by regulating the expression of NEMO and activation of IL-6/STAT3 signaling subsequently

leading to the expression of a tumor suppressive protein, PML (Fig 7). Due to heterogeneity in DCIS and a small sample size used in our studies, our conclusion may hold true for a subset of ER^+/PR^+ breast cancers. Furthermore, a formal proof that E+P regulation of NEMO plays a protective role in breast cancer requires a model in which E+P is protective against breast cancer and then show that the loss of NEMO in that model resulted in loss of E+P protection against breast cancer.

Supplementary Material

Refer to Web version on PubMed Central for supplementary material.

Acknowledgments

Financial support: This work was supported by NCI 1K22 CA160587-01A1 to K.E. Valdez, NCI K99/R00 CA127462 to F. Behbod, NCI Cancer Center Support Grant (CCSG) P30 CA168524 to All authors, CPRIT (Cancer Prevention and Research Institute of Texas) RP150232 to D.P. Edwards, and CCSG's Biospecimen Shared Resource (BSR) to all authors. The University of Kansas Medical Center Flow Cytometry Core Facility is sponsored by the NIH/NIGMS COBRE grant P30 GM103326 to all authors.

We like to acknowledge the University of Kansas Medical Center Flow Cytometry Core Facility director, Mr. Richard Hastings for his superb technical assistance and guidance with our studies.

References

1. Allegra CJ, Aberle DR, Ganschow P, Hahn SM, Lee CN, Millon-Underwood S, et al. National Institutes of Health State-of-the-Science Conference statement: Diagnosis and Management of Ductal Carcinoma In Situ September 22–24, 2009. J Natl Cancer Inst. 2010; 102(3):161–9. [PubMed: 20071686]
2. Virnig BA, Tuttle TM, Shamliyan T, Kane RL. Ductal carcinoma in situ of the breast: a systematic review of incidence, treatment, and outcomes. J Natl Cancer Inst. 2010; 102(3):170–8. [PubMed: 20071685]
3. Leonard GD, Swain SM. Ductal carcinoma in situ, complexities and challenges. J Natl Cancer Inst. 2004; 96(12):906–20. [PubMed: 15199110]
4. Valdez KE, Fan F, Smith W, Allred DC, Medina D, Behbod F. Human primary ductal carcinoma in situ (DCIS) subtype-specific pathology is preserved in a mouse intraductal (MIND) xenograft model. J Pathol. 2011; 225(4):565–73. [PubMed: 22025213]
5. Ewertz M, Duffy SW, Adami HO, Kvale G, Lund E, Meirik O, et al. Age at first birth, parity and risk of breast cancer: a meta-analysis of 8 studies from the Nordic countries. Int J Cancer. 1990; 46(4):597–603. [PubMed: 2145231]
6. Lambe M, Hsieh C, Trichopoulos D, Ekbom A, Pavia M, Adami HO. Transient increase in the risk of breast cancer after giving birth. N Engl J Med. 1994; 331(1):5–9. [PubMed: 8202106]
7. Rosner B, Colditz GA, Willett WC. Reproductive risk factors in a prospective study of breast cancer: the Nurses' Health Study. Am J Epidemiol. 1994; 139(8):819–35. [PubMed: 8178795]
8. Colditz GA, Rosner B. Cumulative risk of breast cancer to age 70 years according to risk factor status: data from the Nurses' Health Study. Am J Epidemiol. 2000; 152(10):950–64. [PubMed: 11092437]
9. Nelson HD, Zakher B, Cantor A, Fu R, Griffin J, O'Meara ES, et al. Risk factors for breast cancer for women aged 40 to 49 years: a systematic review and meta-analysis. Ann Intern Med. 2012; 156(9):635–48. [PubMed: 22547473]
10. Ritte R, Tikk K, Lukanova A, Tjonneland A, Olsen A, Overvad K, et al. Reproductive factors and risk of hormone receptor positive and negative breast cancer: a cohort study. BMC Cancer. 2013; 13:584. [PubMed: 24321460]

11. Ritte R, Lukanova A, Tjonneland A, Olsen A, Overvad K, Mesrine S, et al. Height, age at menarche and risk of hormone receptor-positive and -negative breast cancer: a cohort study. Int J Cancer. 2013; 132(11):2619–29. [PubMed: 23090881]
12. Rajkumar L, Kittrell FS, Guzman RC, Brown PH, Nandi S, Medina D. Hormone-induced protection of mammary tumorigenesis in genetically engineered mouse models. Breast Cancer Res. 2007; 9(1):R12. [PubMed: 17257424]
13. Mohammed H, Russell IA, Stark R, Rueda OM, Hickey TE, Tarulli GA, et al. Progesterone receptor modulates ERalpha action in breast cancer. Nature. 2015; 523(7560):313–7. [PubMed: 26153859]
14. Daniel AR, Gaviglio AL, Knutson TP, Ostrander JH, D'Assoro AB, Ravindranathan P, et al. Progesterone receptor-B enhances estrogen responsiveness of breast cancer cells via scaffolding PELP1- and estrogen receptor-containing transcription complexes. Oncogene. 2015; 34(4):506–15. [PubMed: 24469035]
15. Welm BE, Dijkgraaf GJ, Bledau AS, Welm AL, Werb Z. Lentiviral transduction of mammary stem cells for analysis of gene function during development and cancer. Cell Stem Cell. 2008; 2(1):90–102. [PubMed: 18371425]
16. Behbod F, Kittrell FS, LaMarca H, Edwards D, Kerbawy S, Heestand JC, et al. An intraductal human-in-mouse transplantation model mimics the subtypes of ductal carcinoma in situ. Breast Cancer Res. 2009; 11(5):R66. [PubMed: 19735549]
17. Elsarraj HS, Hong Y, Valdez KE, Michaels W, Hook M, Smith WP, et al. Expression profiling of in vivo ductal carcinoma in situ progression models identified B cell lymphoma-9 as a molecular driver of breast cancer invasion. Breast Cancer Res. 2015; 17:128. [PubMed: 26384318]
18. Fisman EZ, Tenenbaum A. The ubiquitous interleukin-6: a time for reappraisal. Cardiovascular diabetology. 2010; 9:62. [PubMed: 20937099]
19. Sansone P, Storci G, Tavolari S, Guarnieri T, Giovannini C, Taffurelli M, et al. IL-6 triggers malignant features in mammospheres from human ductal breast carcinoma and normal mammary gland. J Clin Invest. 2007; 117(12):3988–4002. [PubMed: 18060036]
20. Scheller J, Rose-John S. Interleukin-6 and its receptor: from bench to bedside. Medical microbiology and immunology. 2006; 195(4):173–83. [PubMed: 16741736]
21. Sullivan NJ, Sasser AK, Axel AE, Vesuna F, Raman V, Ramirez N, et al. Interleukin-6 induces an epithelial-mesenchymal transition phenotype in human breast cancer cells. Oncogene. 2009; 28(33):2940–7. [PubMed: 19581928]
22. Lee SO, Chun JY, Nadiminty N, Lou W, Gao AC. Interleukin-6 undergoes transition from growth inhibitor associated with neuroendocrine differentiation to stimulator accompanied by androgen receptor activation during LNCaP prostate cancer cell progression. Prostate. 2007; 67(7):764–73. [PubMed: 17373716]
23. Hubackova S, Krejcikova K, Bartek J, Hodny Z. Interleukin 6 signaling regulates promyelocytic leukemia protein gene expression in human normal and cancer cells. J Biol Chem. 2012; 287(32):26702–14. [PubMed: 22711534]
24. Xie X, Rigor P, Baldi P. MotifMap: a human genome-wide map of candidate regulatory motif sites. Bioinformatics. 2009; 25(2):167–74. [PubMed: 19017655]
25. Orange JS, Geha RS. Finding NEMO: genetic disorders of NF-[kappa]B activation. J Clin Invest. 2003; 112(7):983–5. [PubMed: 14523034]
26. Senftleben U, Cao Y, Xiao G, Greten FR, Krahn G, Bonizzi G, et al. Activation by IKKalpha of a second, evolutionary conserved, NF-kappa B signaling pathway. Science. 2001; 293(5534):1495–9. [PubMed: 11520989]
27. Lee TH, Huang Q, Oikemus S, Shank J, Ventura JJ, Cusson N, et al. The death domain kinase RIP1 is essential for tumor necrosis factor alpha signaling to p38 mitogen-activated protein kinase. Mol Cell Biol. 2003; 23(22):8377–85. [PubMed: 14585994]
28. Festjens N, Vanden Berghe T, Cornelis S, Vandenabeele P. RIP1, a kinase on the crossroads of a cell's decision to live or die. Cell Death Differ. 2007; 14(3):400–10. [PubMed: 17301840]
29. Salomoni P, Pandolfi PP. The role of PML in tumor suppression. Cell. 2002; 108(2):165–70. [PubMed: 11832207]

30. Kondylis V, Polykratis A, Ehlken H, Ochoa-Callejero L, Straub BK, Krishna-Subramanian S, et al. NEMO Prevents Steatohepatitis and Hepatocellular Carcinoma by Inhibiting RIPK1 Kinase Activity-Mediated Hepatocyte Apoptosis. Cancer Cell. 2015; 28(5):582–98. [PubMed: 26555174]
31. Liu XY, Lai F, Yan XG, Jiang CC, Guo ST, Wang CY, et al. RIP1 Kinase Is an Oncogenic Driver in Melanoma. Cancer Res. 2015; 75(8):1736–48. [PubMed: 25724678]
32. Gyorffy B, Lanczky A, Eklund AC, Denkert C, Budczies J, Li Q, et al. An online survival analysis tool to rapidly assess the effect of 22,277 genes on breast cancer prognosis using microarray data of 1,809 patients. Breast Cancer Res Treat. 2010; 123(3):725–31. [PubMed: 20020197]
33. Shostak K, Chariot A. NF-kappaB, stem cells and breast cancer: the links get stronger. Breast Cancer Res. 2011; 13(4):214. [PubMed: 21867572]
34. Hoesel B, Schmid JA. The complexity of NF-kappaB signaling in inflammation and cancer. Mol Cancer. 2013; 12:86. [PubMed: 23915189]
35. Decker T, Kovarik P. Serine phosphorylation of STATs. Oncogene. 2000; 19(21):2628–37. [PubMed: 10851062]
36. Chlebowski RT, Kuller LH, Prentice RL, Stefanick ML, Manson JE, Gass M, et al. Breast cancer after use of estrogen plus progestin in postmenopausal women. N Engl J Med. 2009; 360(6):573–87. [PubMed: 19196674]
37. Chlebowski RT, Anderson G, Manson JE, Pettinger M, Yasmeen S, Lane D, et al. Estrogen alone in postmenopausal women and breast cancer detection by means of mammography and breast biopsy. J Clin Oncol. 2010; 28(16):2690–7. [PubMed: 20439627]
38. Hunter DJ, Colditz GA, Hankinson SE, Malspeis S, Spiegelman D, Chen W, et al. Oral contraceptive use and breast cancer: a prospective study of young women. Cancer Epidemiol Biomarkers Prev. 2010; 19(10):2496–502. [PubMed: 20802021]
39. Ailles LE, Weissman IL. Cancer stem cells in solid tumors. Curr Opin Biotechnol. 2007; 18(5):460–6. [PubMed: 18023337]
40. Singhal H, Greene ME, Tarulli G, Zarnke AL, Bourgo RJ, Laine M, et al. Genomic agonism and phenotypic antagonism between estrogen and progesterone receptors in breast cancer. Sci Adv. 2016; 2(6):e1501924. [PubMed: 27386569]
41. Vignon F, Bardon S, Chalbos D, Rochefort H. Antiestrogenic effect of R5020, a synthetic progestin in human breast cancer cells in culture. J Clin Endocrinol Metab. 1983; 56(6):1124–30. [PubMed: 6682424]
42. Chen CC, Hardy DB, Mendelson CR. Progesterone receptor inhibits proliferation of human breast cancer cells via induction of MAPK phosphatase 1 (MKP-1/DUSP1). J Biol Chem. 2011; 286(50):43091–102. [PubMed: 22020934]
43. Kabos P, Finlay-Schultz J, Li C, Kline E, Finlayson C, Wisell J, et al. Patient-derived luminal breast cancer xenografts retain hormone receptor heterogeneity and help define unique estrogen-dependent gene signatures. Breast Cancer Res Treat. 2012; 135(2):415–32. [PubMed: 22821401]
44. Piazza F, Gurrieri C, Pandolfi PP. The theory of APL. Oncogene. 2001; 20(49):7216–22. [PubMed: 11704849]
45. Guan D, Kao HY. The function, regulation and therapeutic implications of the tumor suppressor protein, PML. Cell Biosci. 2015; 5:60. [PubMed: 26539288]
46. Narita M, Nunez S, Heard E, Narita M, Lin AW, Hearn SA, et al. Rb-mediated heterochromatin formation and silencing of E2F target genes during cellular senescence. Cell. 2003; 113(6):703–16. [PubMed: 12809602]

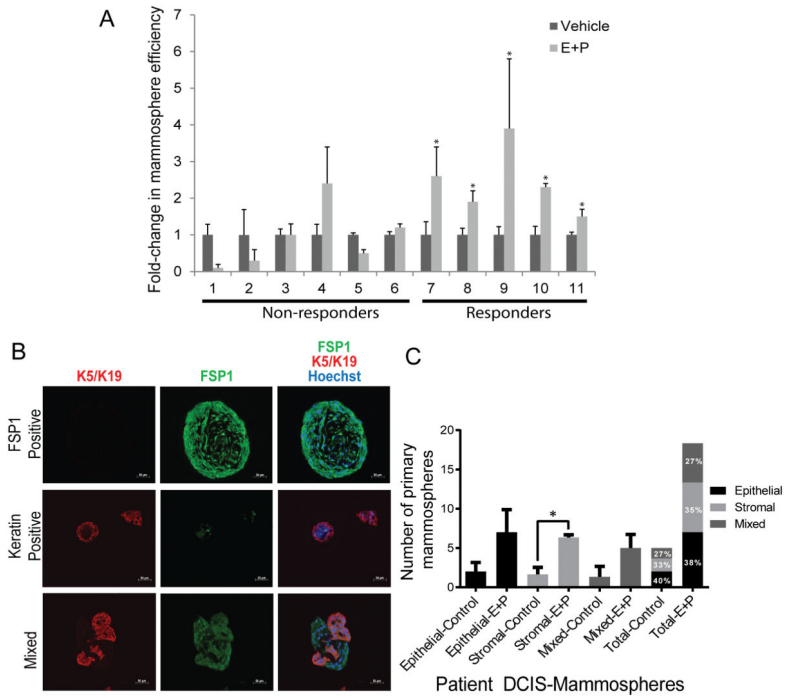

Figure 1.

Only a subset of patient-derived ER+/PR+ DCIS cells responded to hormone treatment *in vitro* by increasing mammosphere formation efficiency. (A) Only a subset of cases responded to steroid hormone treatment *in vitro* by increasing mammosphere-forming efficiency (cases 7–11). Data are presented as mean± SEM. (*indicates E+P increased mammosphere efficiency compared to vehicle control, P<0.05). (B) Representative IF images of primary mammospheres from three patient biopsies embedded in paraffin. FSP1 is shown in green (Fibroblast marker), K5/K19 in red (Epithelial marker), and Hoechst in blue, demonstrating the appearance of stromal (FSP1 positive), epithelial (keratin positive), and mixed stromal and epithelial mammospheres (mixed). (C) Bar graph representing quantification of epithelial-derived, stromal derived, and mixed epithelial and stromal derived mammospheres, comparing E+P treated to control. The data represent the mean ± SEM (n=3, *P<0.05).

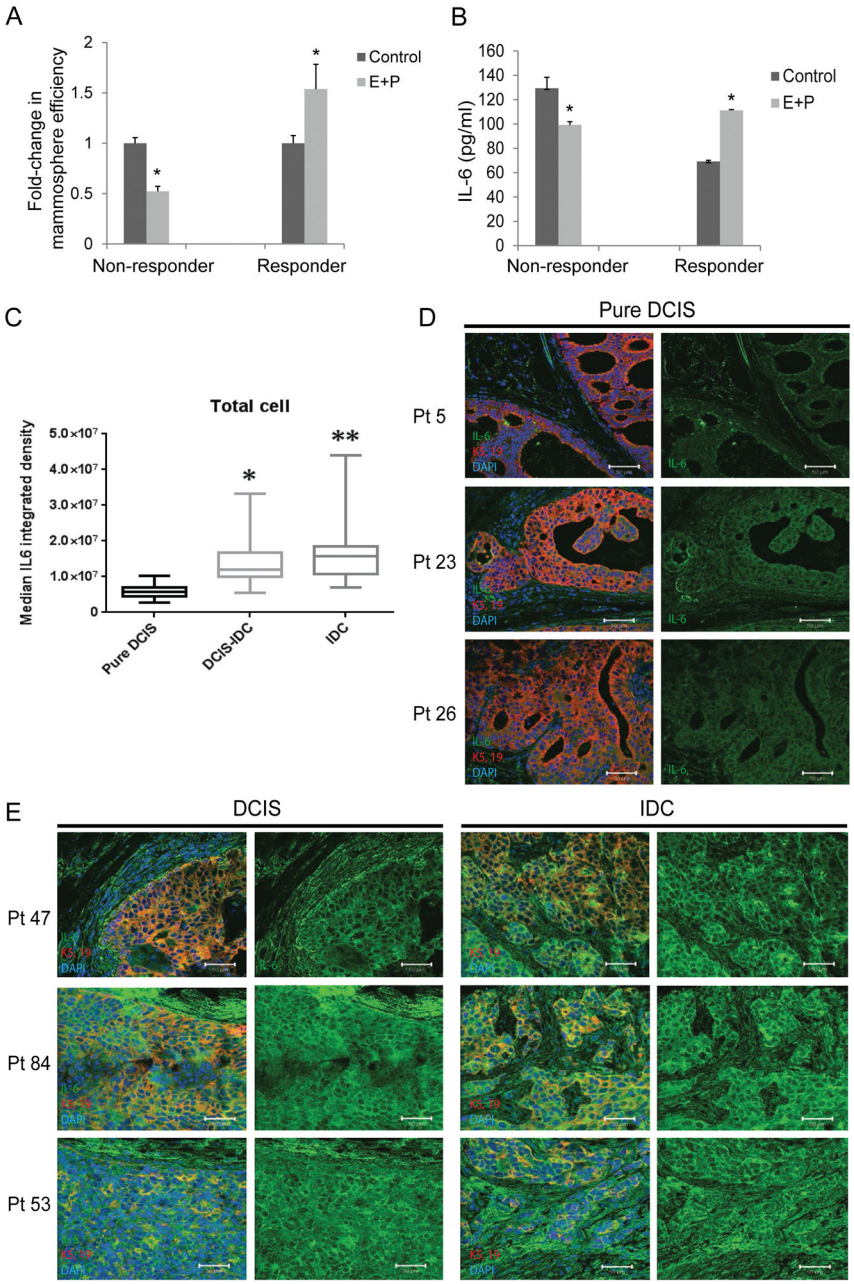

Figure 2.

E+P treatment of patient derived DCIS cells results in increased mammosphere efficiency *in vitro* and increased IL-6 expression as a function of invasive progression in patients' DCIS. (A) Graph depicts mammosphere formation efficiency in representative cases of non-responders (3 total cases examined) and a responder (1 total case examined), and (B) corresponding IL-6 secretion as measured by ELISA of the cell culture media (*P<0.05 compared to vehicle control). (C) Boxplots showing the distribution of IL-6 expression from 30 cases of pure DCIS and 60 cases of DCIS with IDC. A two-sample t-test was used to compare expression in pure DCIS to expression in DCIS with associated with IDC.

Expression was higher in DCIS with associated IDC compared to pure DCIS. On DCIS with associated IDC samples, IL-6 expression was also significantly higher when comparing DCIS regions to the corresponding IDC regions using a paired t-test. IL-6 expression levels were quantified using Metamorph. (D) Representative images of pure DCIS stained for IL-6 (green) and K-5 and-19 (red). (E) Representative images from patients with both DCIS (left) and IDC (right), stained for IL-6 (green) and K-5 and-19 (red).

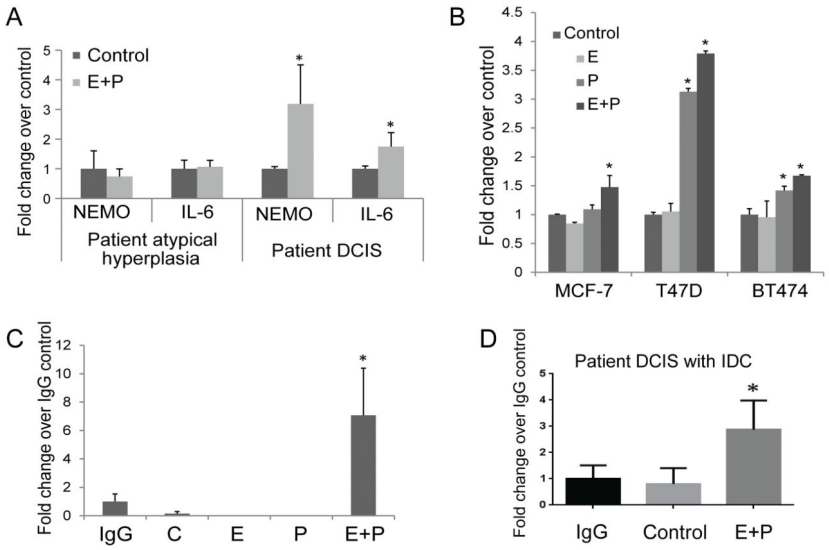

Figure 3.

(A) Cells from patient samples of atypical hyperplasia and DCIS were cultured under non-adherent conditions for 1 week in the presence of vehicle, E (10nM), P (100nM), or E+P. NEMO and IL-6 gene expression was measured by qPCR. (B) ER+PR+ breast cancer cells were cultured as monolayers for 12 hours in the presence of vehicle, E (10 nM), P (10nM), or E+P. NEMO gene expression was measured by qPCR. Data are presented as mean± SEM. * $P < 0.05$ compared to vehicle control. ChIP assays were performed on MCF7 breast cancer cells (C) and on primary patient DCIS with IDC (D) treated with vehicle, E (10nM), P (10nM), or E+P for 1h. Immunoprecipitation was performed using an anti-ER antibody and qPCR was performed using primers targeting the potential ERE within the *IKBKG* promoter region. Data is presented as mean± SEM. * $P<0.05$ compared to IgG control.

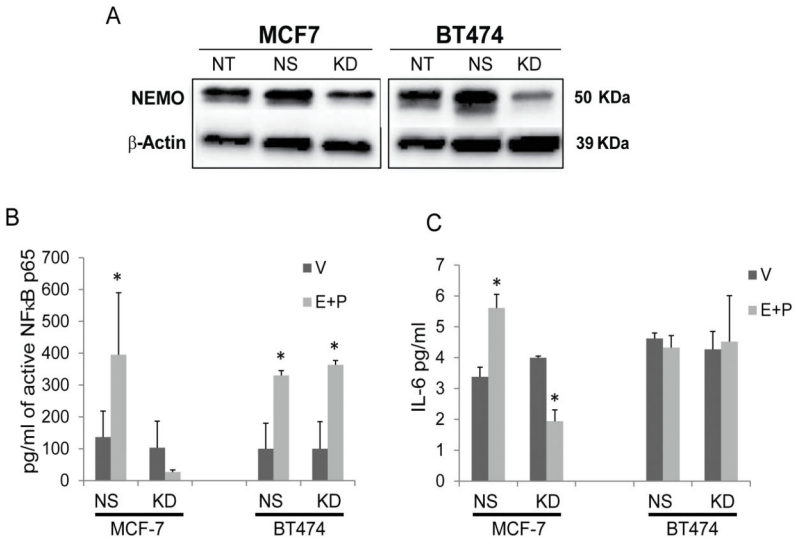

Figure 4.

NEMO is required for the E+P-induced increase in NFκB activation and IL-6 secretion in ER+PR+ breast cancer cells. (A) Western analysis was used to confirm knock down of NEMO in MCF7 and BT474. NT: non-transduced control. NS: scrambled non-silencing control. KD: NEMO-targeting shRNA. (B) MCF7 and BT474 cells were serum-starved for 24h before treatment with 10nM E and 10nM P. Nuclear extract was collected 48 h later and NFκB p65 activity within the nucleus was measured. * P<0.05 compared to vehicle (V) control. (C) MCF7 and BT474 cells were serum-starved for 24 h before treatment with 10nM E and 10nM P. Cell culture media was collected 48h later and IL-6 secretion was measured by ELISA. * P<0.05 compared to vehicle (V) control.

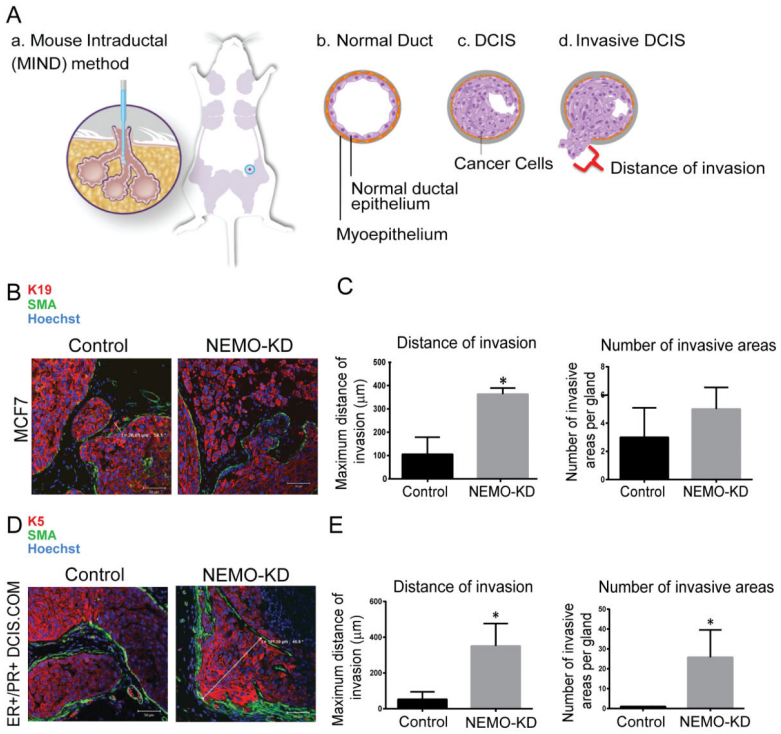

Figure 5.

NEMO-KD DCIS lesions showed increased *in vivo* invasive progression. (A) MIND is a transplantation technique that involves intraductal injection of DCIS cells into the primary mouse mammary ducts (a). (b) Normal mammary ducts include a single layer of ductal epithelium surrounded by a layer of myoepithelium. (c) Ductal carcinoma in situ (DCIS) refers to *in situ* or non-invasive breast cancer in which cancer cells are contained within the boundaries of the myoepithelial layer and the basement membrane. (d) Invasive DCIS refers to DCIS lesions in which the cancer cells have bypassed the normal boundaries of the myoepithelial layer and have invaded the surrounding stroma. Invasive DCIS is assessed by counting the number of invasive DCIS lesions per high power field as well as the maximum distance traveled by the cancer cells beyond the mammary ductal system; indicated by the red bracket in (d). Glands from control and NEMO-KD MCF7 (B and C) and ER+/PR+ DCIS.com (D and E) MIND xenografts were collected at 6 and 8 weeks post-intraductal injection, respectively. IF staining of K5/19 (red), SMA (green), and hoechst (blue) in MCF7 (B) and ER+/PR+ DCIS.com (D) MIND demonstrating how distance of invasion was measured. (C and E) Bar graphs represent the maximum distance of invasion and number of invasive lesions in control and NEMO KD for MCF7 (C) and ER+/PR+ DCIS.com (E) MIND xenografts. Data represent the mean ± SEM. (n=4, *P<0.05).

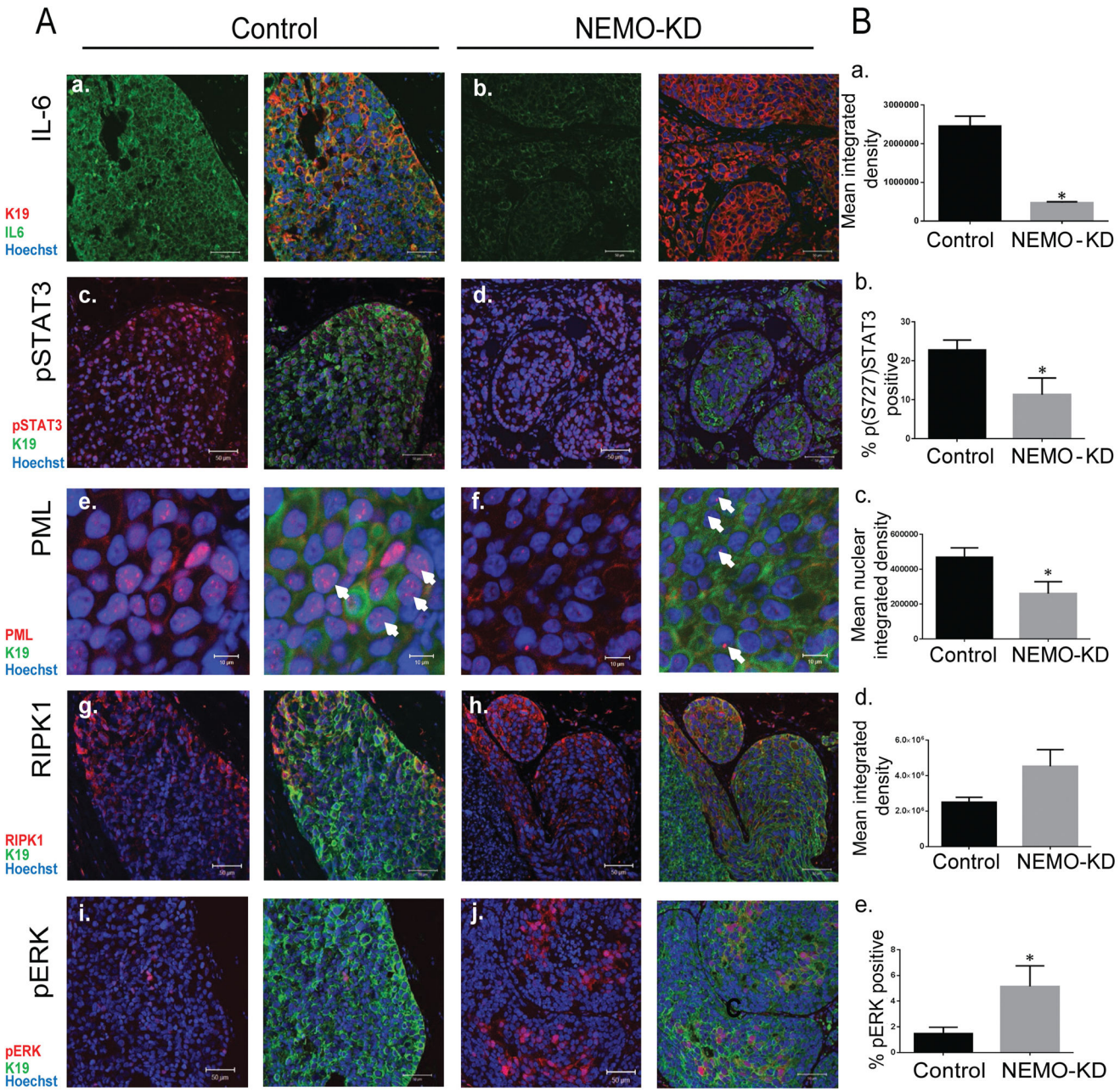

Figure 6.

NEMO-KD DCIS lesions showed a significant reduction in IL-6 signaling and PML expression. Glands from control and NEMO-KD MCF7 MIND xenografts were collected at 6 weeks post-intraductal injection and expression of different markers in NEMO-KD MIND xenografts were measured. (A) IF images of control (a,c,e,g, and i) and NEMO-KD MCF7 (b,d,f,h, and j) xenografts stained with IL-6 (a and b) shown in green, pSTAT3 (c and d) in red, PML (e and f) in red, RIPK1 (g and h) in red and pERK (i and j) in red, K19 shown in green, and hoechst in blue. Scale bars=50μm (10μm for PML images), 40x magnification. The white arrows point to the PML nuclear bodies (B) Bar graphs of fluorescence intensity units for IL-6 (a), pSTAT3 (b), PML (c), RIPK1 (d) and p-ERK (e) in control and NEMO-

KD MCF7 cells. Measurements were obtained by Metamorph. The data represent the mean ±SEM (n=4, *P<0.05).

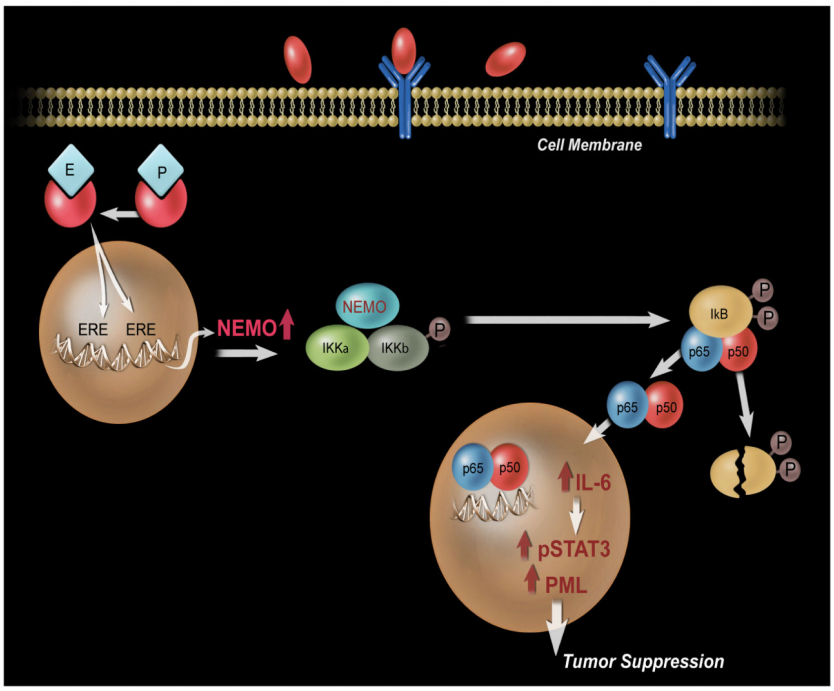

Figure 7.

An illustration of mechanism by which E+P may protect against aggressive breast cancer. E +P increases ER binding to the *IKBKG* promoter and results in increased NEMO expression. NEMO is the regulatory subunit of the IKK (inhibitor of NF-kappa-B kinase) core complex, which phosphorylates the inhibitor of NF-kappa-B (IκB) thus promoting the dissociation of the IκB and ultimately degradation of the inhibitor and subsequent activation and nuclear translocation of NFκB. NF-κB signaling promotes NFκB target gene transcription, including IL-6, and activation of IL-6/STAT3 signaling subsequently leading to the expression of a tumor suppressive protein, PML.